



Tissue strain rate estimator using ultrafast IQ complex data

Redouane Ternifi, Melouka Elkateb Hachemi, Jean-Pierre Remenieras

► To cite this version:

Redouane Ternifi, Melouka Elkateb Hachemi, Jean-Pierre Remenieras. Tissue strain rate estimator using ultrafast IQ complex data. Acoustics 2012, Apr 2012, Nantes, France. hal-00810913

HAL Id: hal-00810913

<https://hal.science/hal-00810913>

Submitted on 23 Apr 2012

HAL is a multi-disciplinary open access archive for the deposit and dissemination of scientific research documents, whether they are published or not. The documents may come from teaching and research institutions in France or abroad, or from public or private research centers.

L'archive ouverte pluridisciplinaire **HAL**, est destinée au dépôt et à la diffusion de documents scientifiques de niveau recherche, publiés ou non, émanant des établissements d'enseignement et de recherche français ou étrangers, des laboratoires publics ou privés.



Tissue strain rate estimator using ultrafast IQ complex data

R. Ternifi^{a,b}, M. Elkateb Hachemi^a and J.-P. Remenieras^a

^aUMR U930 CNRS ERL 3106, 10 Bd Tonnelle Batiment Vialle Equipe 5 INSEM, 37032
Tours, France, France

^bLaboratoire de Biomécanique et Mécanique des Chocs, IFSTTAR UMR_T9406 25 avenue
François Mitterrand 69675 Bron
redouane.ternifi@etu.univ-tours.fr

In order to study fast deformations of tissues such as brain pulsatility or artery wall motion, ultrafast transient elastography processing is used to estimate the strain field by tracking the natural tissue displacements over time. In this study, transient motion of carotid tissue was estimated using an ultrafast imaging system. The strain was computed directly from the ultrafast in-phase (I) and quadrature-phase (Q) complex data using the extended autocorrelation strain estimator (EASE). The EASE provides high SNRe regardless of depth and avoids the elastographic noise due to the gradient operation generally used to estimate the strain field. The developed algorithm was validated *in vitro* using a free hand compression applied on an acoustic phantom with a hard inclusion. *In vivo* experiments were then carried out to evaluate the strain of the carotid artery wall and adjacent regions. Ultrasound data were acquired at 7.5 MHz with 500 Hz frame rate. The estimated displacement velocity and strain values of the wall artery were 2.5 cm/s, and 60% respectively. The values for the adjacent region were 1.5 cm/s and 20% respectively. In the future, a study will be conducted to test the feasibility of using EASE to assess brain tissue pulsatility.

1 Introduction

Historically, in the biomedical field, ultrasound has been mostly used to image the anatomic structure of tissues and to measure of blood flow. In the last twenty years, considerable research effort has been invested in the development of techniques for measuring the movements of solid tissue. In parallel, much work has been devoted to the development of magnetic resonance phase imaging techniques for measuring brain tissue movements and associated hydrodynamics [1]. The movements were directed caudally, medially and posteriorly in the basal ganglia, and caudally-anteriorly in the pons. The resultant brain movement was found to be funnel shaped, as if the brain were pulled by the spinal cord. The total intracranial content of arterial blood, venous blood, capillary blood (brain volume) and cerebrospinal fluid (CSF) remains essentially constant at every moment of the pulsatile cardiac cycle. The increase in brain volume is followed by the release of the CSF into the cranial cavity at the foramen magnum. Expansion of the brain takes place when intracranial pressure is below spinal CSF pressure. This volume increase is associated with deformations of the cerebral tissue. In this study, we want to develop an ultrasound imaging method suitable to measure the natural tissue strain during cardiac cycle. Different elastography techniques were developed to measure mechanical characteristics of tissue. Strain measurement coupled with static or dynamic external compression of the tissue [2, 3, 4], measurement of the natural pulsatile motion of tissue due to blood flow [5, 6, 7] or measurement of tissue displacement and strain of the myocardium to assess myocardial viability [8, 9]. In more recent years, these techniques have been extended to measure the deformation of tissue around arteries due to the internal blood pressure to study vascular dynamics [10].

In literature, two techniques are commonly used to estimate the deformation of biological tissues: time delay estimators based on intercorrelation methods applied on radiofrequency (RF) US lines and Doppler techniques based on time domain mean frequency estimators.

In this study, we focused on investigating the natural motion and strain of the carotid artery wall and the surrounding tissue using an ultrafast US system providing an acquisition as IQ complex signals. However, to estimate the deformation we used an extended autocorrelation strain estimator which is adapted to IQ signals.

IQ signal is sampled at the centre frequency of the emission signal (in our case 7.5 MHz). In these conditions, it was not easy to apply the intercorrelation method. In fact, with this sampling rate the Shannon limit was not respected, it was not even possible to describe correctly the RF signal. Consequently we have chosen to use autocorrelation techniques for our estimation. The limitation of the autocorrelation techniques for large deformations was overcome by using a high frame rate (the frame rate of the system is 100 to 5000 frames/second). With such rapid frame rates, we can estimate precisely the change in the phase of the autocorrelation function over several frames.

The aim of this study is to obtain the 2D through-thickness strain in a deformed medium with ultrafast acquisition. However, the displacement tracking was performed separately for acoustic signatures over the time acquisition in order to estimate directly the strain field from IQ images.

2 Materiel and methods

2.1 Data acquisitions

Ultrasound acquisitions were performed by an Aixplorer Ultrafast Scanner (SuperSonic Imagine) using a SuperLinearTM probe (Civco SL 15-4) composed of 256 elements. With this system it is possible to access the beamformed demodulated complex in-phase (I) and quadrature-phase (Q) signals. This signal is sampled at the centre frequency of the probe, i.e. 7.5 MHz, which means that the spatial resolution is equal to a half wavelength (100 μ m). The I and Q signals are saved in a vector in this order: I(1) Q(1) I(2) Q(2)...I(n) Q(n) ranked by increasing depth then by increasing azimuth (lateral dimension). From this vector, a 3D matrix IQ(m,l,n) is created with m a depth index varying from 0 to M where M is the total number of samples per IQ line. Then, l is a lateral index varying from 1 to L where L is the number of signal lines per frame. Finally, n is a frame index varying from 1 to N where N the total number of frames (Figure 1).

IQ complex data was acquired on a 3 cm depth by 4 cm wide window on a elastic phantom (344 samples / 256 lines) with a frame rate of 500 images/s. 1000 frames were acquired giving a total of 2 seconds of acquisition.

A manual compression was applied on the phantom with the probe to create a quasi-static motion in the phantom. Velocity of displacement and strain in the phantom were estimated offline with MATLAB (R2010a) using the methods described previously. The length for each IQ sample volume was 1.508 mm and the center-to-center spacing of each IQ sample volume was 0.377 mm.

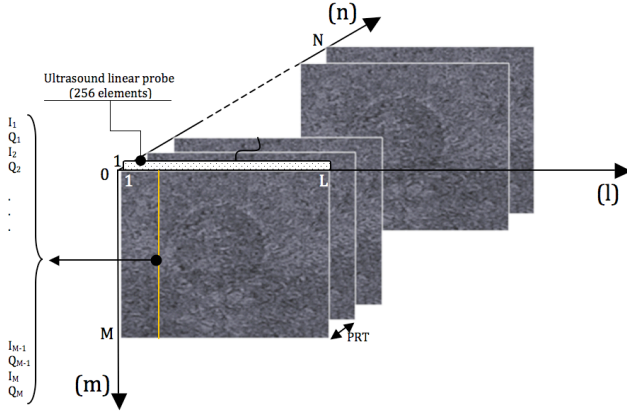


Figure 1: Ultrafast (IQ) imaging. A 7.5 MHz linear ultrasound probe (256 elements) was used for 2D scan, i.e. (MxL) ultrasound image. The ultrafast system allowed to acquire N (IQ) images with a PRF (1/PRT) of 1000 Hz. 3D data was then stored for N images and each (IQ) image was composed from L (IQ) signal corresponding to a vector with real and imaginary parts of signal complex amplitudes.

2.2 Tissue motion algorithms

The algorithms developed in this work are based on autocorrelation techniques to estimate displacement velocity of tissue induced by the natural pulsatile motion of the carotid wall due to blood flow. However, local velocities may be influenced by either overall heart motion or by motion induced by contraction in adjacent segments [11]. For this reason, the strain and strain rate which describe only local changes were also estimated.

As explained before, the strain is calculated directly for IQ signals. The demodulated signal IQ at a certain lateral position can be written as:

$$IQ(m,n) = I(m,n) + jQ(m,n) = A(m,n)e^{j\phi(m,n)} \quad (1)$$

where A is the amplitude of signal and $\phi(m,n)$ the phase of the signal returned from the m^{th} depth and the n^{th} pulse.

The velocity estimator was defined in Eq. (2). It is an extension of the autocorrelation estimator developed by Hoeks *et al.* in 1994 [12]. This estimates the mean velocity using multiple, spatially contiguous IQ sample volumes in time. This approach increases the accuracy of the velocity estimate at the expense of decreasing spatial resolution. It is expressed mathematically as:

$$V(m,n) = \frac{\lambda}{4\pi T} \text{Arg} \left\{ \sum_{a=0}^{Lapz} \sum_{b=0}^{Lapt} S(m-a,n-b) S^*(m-a,n-b-1) \right\} \quad (2)$$

where λ is the wavelength in the tissue, T is the time interval between two acquisitions. Lapz is the number of samples defining the volume of interest. Lapt is the number of temporal samples in the autocorrelation over which the mean velocity is estimated.

EASE method permits to obtain the strain from IQ samples as expressed in Eq. (3): a first autocorrelation is applied at each depth over a set of successive temporal IQ pairs. This estimates the mean change in phase over time, which is proportional to the velocity or displacement. A second autocorrelation is then performed on the results of the first one, which corresponds to the estimation of the mean changes in phase over the depth. This result is proportional to the strain rate.

$$\varepsilon(m,n) = \frac{\lambda}{4\pi Ds} \text{Arg} \sum_{a=0}^{Lapz} \left\{ \sum_{b=0}^{Lapt} S(m-a-1,n-b) S^*(m-a-1,n-b-1) \right\} \times \left\{ \sum_{b=0}^{Lapt} S(m-a,n-b) S^*(m-a,n-b-1) \right\}^* \quad (3)$$

3 Results and discussion

3.1 In vitro experiment

A uniformly elastic phantom (CIRS, Model 049) with a single inclusion (Type IV) was used to carry out a freehand elastography test. The ultrasound probe was used to apply a quasi-static compression over the inclusion zone. The ultrafast acquisition allowed 3D data with a PRF of 500 Hz to be obtained. Displacements were deduced from velocity calculation in the first step of EASE in the temporal plane IQ(MxN). Spatial displacement in axial plane (MxL) could be presented at the end of processing. Then the local strain rate images were calculated in the second step of EASE algorithm and could be also presented in the axial plane. Finally, addition of local strain images was performed to obtain a cumulated strain rate image (elastogram). In this case, high strain rate values were reached *i.e.* an elastogram with a good contrast and high elastographic signal to noise ratio [14].

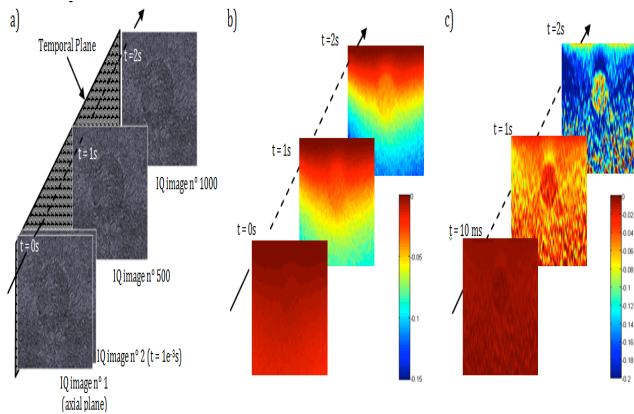


Figure 2: a) IQ Ultrafast imaging: 2s acquisition with a PRF = 500 Hz (500 images/s), b) Gradient of spatial displacement and c) Elastograms obtained using the EASE.

Figure 2-a shows B-mode images from the elastic phantom acquired for 2s with a temporal step of 2ms. The inclusion shape is clearly seen in the centre of the image. Figure 2-b shows the cumulated displacement at different times: at 10ms (the beginning of the compression), at 1s and at 2s (the end of the compression). One can see in these images the gradient of displacement through the depth. The compression was applied by the ultrasound probe on the bottom, thus regions near the probe moved with a displacement close to the probe motion, which corresponds to low displacement values. In contrast, the distance between deep zones and the probe decreased with compression, which explains the high displacement values. Furthermore, around the inclusion zone, the gradient was higher above the inclusion due to the force and lower below due to the hardness of the inclusion *i.e.* the inclusion is less deformed. Displacement images clearly describe the temporal evolution of the compression. At the beginning of the compression, a very slight displacement, At 1s, the maximum of displacement exceeded to 0.08 cm and at the end of the compression the maximum reached to 0.15 cm.

In Figure 2-c, the EASE was used to calculate the strain rate images that were cumulated over time. In this case, one can see clearly the difference between the inclusion and the background deformation with values of 6 % and 20 % respectively at the end of the compression.

Finally, these results showed clearly the good performance of the EASE estimator to distinctly depict the inhomogeneous deformation in the phantom.

3.2 A. *In vivo* experiment

Velocity of displacements and cumulated strain were estimated on the artery wall (Figure 3 - ROI 1) and adjacent regions (Figure 3 - ROI 2). The estimated velocity of displacement and cumulated strain of the wall artery were ~ 2.5 cm/s, and ~ 60 % respectively while for the adjacent region they were ~ 1.5 cm/s and ~ 20 % respectively. The algorithms were efficient to measure large motions (carotid wall) as well as small motion (regions near the surface of the probe).

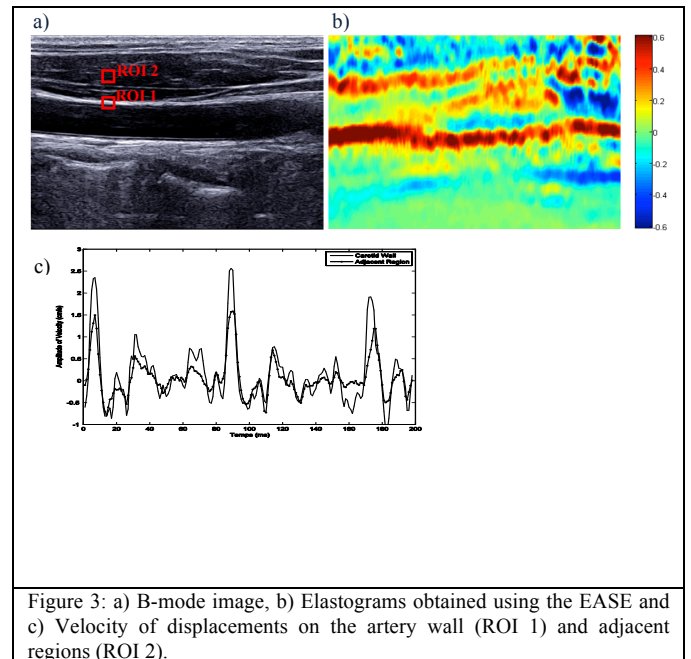


Figure 3: a) B-mode image, b) Elastograms obtained using the EASE and c) Velocity of displacements on the artery wall (ROI 1) and adjacent regions (ROI 2).

Figure 3-a shows the B-mode image obtained from human carotid. The computed elastogram is presented in figure 3-b. It's clear from this elastogram, the artery wall is deformed due to high blood pressure (systole). In figure 3-c we observed high velocity values of carotid artery wall due to high blood pressure (systole). After that, this region return to rest position (diastole). The same behaviour is observed on the adjacent region with smaller amplitude.

Although our results demonstrate the feasibility of *in vivo*, two-dimensional carotid strain rate estimation by an extended autocorrelation. The strain rate profiles shown may contain information derived from different anatomic regions. Nevertheless, the different phases of the cardiac cycle were distinguished.

4 Conclusion

In this paper, the feasibility of an extended autocorrelation strain estimator (EASE) of the *in vivo* human carotid was shown highlighted. For this, complex data sets with high temporal resolution were acquired and subsequently processed to estimate velocity of displacement and strain rate based on an IQ complex algorithm. Results obtained from a gel phantom and artery wall were used to illustrate the good performance of this algorithm. Furthermore, findings showed agree well with those found in the literature. Although many aspects could be improved, these initial results showed that *in vivo* extended strain rate estimation is feasible.

Future work will be to validate the developed algorithms (EASE) for brain tissue motion estimation using an adapted transcranial linear probe.

Acknowledgments: The authors would like to thank PhD, Y. MOFID for helpful discussions and technical assistance and Prof, M. LETHIECQ and PhD Student, C. PLAG for correction of English.

5 References

- [1] D. Greitz, R. Wirestam, A. Franck, B. Nordell, C. Thomsen, F. Stahlberg, "Pulsatile brain movement and associated hydrodynamics studied by magnetic resonance phase imaging", *Diagnostic neuroradiology*, 34, 370-380 (1992).
- [2] L. Gao, K. Parker, R. Lerner, S. Levinson, "Imaging of the elastic properties of tissue". *Ultrasound Med Biol* 22(8), 959-977 (1996).
- [3] J. Ophir, E. Cespedes, H. Ponnekanti, et al. "Elastography: a quantitative method for imaging the elasticity of biological tissues", *Ultrason Imaging* 13(2), 111-134 (1991).
- [4] J. Ophir, K. Alam, B. Garra, et al. "Elastography: ultrasonic estimation and imaging of the elastic properties of tissue". *Proc Inst Mech Eng[H]* 213(H3), 203-233 (1999).
- [5] J. Kucewicz, L. Huang, K. Beach, "Plethysmographic arterial waveform strain discrimination by Fisher's method", *Ultrasound Med Biol* 30(6), 773-782 (2004).
- [6] J. Kucewicz, B. Dunmire, D. Leotta, H. Panagiotides, M. Paun, K. Beach, "Functional tissue pulsatility imaging of the brain during visual stimulation", *Ultrasound Med Biol* 33(5), 681-690 (2007).
- [7] M. Elkateb Hachemi, T. Desmidt, F. Patat, V. Camus, J. Cottier, J. Remenieras, "Natural Brain Tissue Pulsatility measurement: A pilot study in older depressed patients", *Ultrasonic symp.*, pp. 329-332, 2009
- [8] Kanai H, Koiwa Y, Zhang J. Real-time measurements of local myocardium motion and arterial wall thickening. *IEEE Trans Ultrason Ferroelectr Freq Control* 1999;46(5):1229-1241
- [9] M. Kowalski, T. Kakulski, F. Jamal, et al. "Can natural strain and strain rate quantify regional myocardial deformation? A study of healthy subjects", *Ultrasound Med Biol*, 27(8):1087-1097 (2001).
- [10] J. Mai, M. Insana, "Strain imaging of internal deformation", *Ultrasound Med Biol*, 28(11-12):1475-1484 (2002).
- [11] S. Urheim, T. Edvardsen, H. Torp, B. Angelsen, O. Smiseth, "Myocardial Strain by Doppler Echocardiography: Validation of a New Method to Quantify Regional Myocardial Function", 102:1158-1164 (2000).
- [12] A. Hoeks, P. Brands, T. Arts, R. Reneman, "Subsample volume processing of Doppler ultrasound signals", *Ultrasound Med Biol*, 20(9):953-965 (1994).
- [13] F. Kallel, J. Ophir, "A least-squares strain estimator for elastography", *Ultrason Imaging*, 19:195-208 (1997).
- [14] T. Varghes, J. Ophir, "Noise reduction using temporal stretching with multicompression averaging", *Ultrasound in Medicine and Biology*, 22, 1043-1052 (1996).